



SAR target detection based on the optimal fractional Gabor spectrum feature

Ling-Bing Peng^{a,c}, Yu-Qing Wang^b, Ying-Pin Chen^{d,e}, Zhen-Ming Peng^{a,*}

^a School of Information and Communication Engineering, University of Electronic Science and Technology of China, Chengdu, 611731, China

^b Changchun Institute of Optics, Fine Mechanics and Physics, Chinese Academy of Sciences, Changchun, 130033, China

^c Institute of Optics and Electronics, Chinese Academy of Sciences, Chengdu, 610209, China

^d School of Mathematical Sciences, University of Electronic Science and Technology of China, Chengdu, 611731, China

^e School of Physics and Information Engineering, Minnan Normal University, Zhangzhou, 363000, China

ARTICLE INFO

Publishing editor: Xin Huang

Keywords:

Optimal fractional Gabor transform (FrGT)

Optimal order

Synthetic aperture radar (SAR) target detection

Time-frequency spectrum analysis

ABSTRACT

In this paper, an algorithm based on a fractional time-frequency spectrum feature is proposed to improve the accuracy of synthetic aperture radar (SAR) target detection. By extending the fractional Gabor transform (FrGT) into two dimensions, the fractional time-frequency spectrum feature of an image can be obtained. In the achievement process, we search for the optimal order and design the optimal window function to accomplish the two-dimensional optimal FrGT. Finally, the energy attenuation gradient (EAG) feature of the optimal time-frequency spectrum is extracted for high-frequency detection. The simulation results show that the proposed algorithm has a good performance in SAR target detection and lays the foundation for recognition.

1. Introduction

The synthetic aperture radar (SAR) image has its own speckle noise. The radiation and geometric features are distorted in image processing, and the details of the target are often lost after SAR image filtering. Conventional image detection methods cannot be applied to SAR target detection, so it is necessary to have a better anti-noise target detection method with high robustness.

As an emerging time-frequency analysis tool, the fractional time-frequency analysis can improve the time-frequency resolution by rotating the time-frequency plane based on the traditional time-frequency analysis. It can also improve the time-frequency distribution of the signal, better detecting the signal mutation point and fine analyzing the local characteristics of the signal, especially for weak SAR target detection with low resolution and a low signal-to-noise ratio. At the same time, the time-frequency rotation characteristics in the fractional domain can better reflect the phase information of SAR images. Li et al. [1] used the traditional time-frequency analysis to detect moving weak targets. The fractional Fourier transform (FrFT) is the basis of fractional time-frequency analysis. Namias [2] put forward the concept of FrFT mathematically for the first time. Ozaktas et al. [3] proposed a discrete algorithm with equivalent computational complexity to the fast Fourier transform. After that, the FrFT algorithm attracted more attention from scholars in signal processing. Chen et al. [4] applied the fractional time-frequency analysis to seismic spectral decomposition for oil and gas exploration, and obtained a certain effect. Sinha et al. [5] completed the time-frequency analysis of seismic signals by combining spectral decomposition with the wavelet transform. Peng et al. [6] applied the generalized S-transform to SAR target detection, and proved that a better

* Corresponding author.

E-mail addresses: penglingbing@std.uestc.edu.cn (L.-B. Peng), wangyuqing@hotmail.com (Y.-Q. Wang), 110500617@163.com (Y.-P. Chen), zmpeng@uestc.edu.cn (Z.-M. Peng).

<https://doi.org/10.1016/j.jnlest.2023.100197>

Received 27 December 2022; Received in revised form 17 February 2023; Accepted 19 April 2023

Available online 6 May 2023

1674-862X/© 2023 The Authors. Publishing services by Elsevier B.V. on behalf of KeAi Communications Co. Ltd. This is an open access article under the CC BY-NC-ND license (<http://creativecommons.org/licenses/by-nc-nd/4.0/>).

detection performance would be achieved by the time-frequency analysis method. Pei and Ding [7] proposed the fractional Hilbert transform, which achieved good results in image edge detection. At present, the fractional time-frequency analysis technology has also been widely used in scientific research and engineering technologies, such as signal detection and parameter estimation, fractional optimal filter design, phase recovery and signal reconstruction, and image processing [8]. He et al. [9] proposed an image de-noising method based on a two-dimensional fractional wavelet transform, which effectively improved the peak signal-to-noise ratio (PSNR) of the output image. Long et al. [10] applied various fractional lower-order time-frequency distribution methods to the machine fault signal. Chen et al. [11] established a detection and micro-Doppler extraction method via short-time FrFT in a sparse domain and it could achieve excellent results. Qian et al. [12] proposed a method called the Gabor Wigner transform based on FrFT, to solve the time-frequency analysis problem of multi-component linear frequency modulation signals in the presence of a low signal-to-noise ratio. Wang et al. [13] proposed a matching pursuit-based sliced Winger higher-order spectra (MP-SWHOS) method to overcome the cross-term issues, which was important in the analysis of hydrocarbon reservoirs. Long et al. [14] used the fractional lower-order S-transform time-frequency filtering algorithm to analyze the machine fault signals. A method named the fractional Gabor transform based on kurtosis maximization (KMFrGT) was proposed. Tian and Peng [15] used the kurtosis maximization (KM) method to determine the optimal order of the fractional Gabor transform (FrGT), which made its performance better in non-stationary signal processing.

The core of the proposed method is to obtain the optimal fractional time-frequency spectrum by using time-frequency rotation characteristics, extracting the energy attenuation gradient (EAG) characteristics, and obtaining the optimal feature profile. Experiments show that the time-frequency aggregation is greatly improved under the constraints of the optimal window. After the optimal order FrGT rotates the time-frequency plane, the loss of phase information is compensated and the loss of details caused by filtering is also compensated, which improves the detection performance. The EAG feature is sensitive to the weak mutation and can achieve high precision results even in low contrast and low signal-to-noise ratio environments. In this paper, the FrGT method is extended into two dimensions. Then the fractional time-frequency spectrum feature of an image can be obtained.

2. Optimal FrGT

2.1. Two-dimensional FrGT

Akan and Önen [16] gave the definition of the traditional Gabor transform. And Candan et al. [17] showed the definition and a series of properties of the FrFT transform in detail. The p th order FrGT of a signal $x(t)$ is defined as

$$GT_{x_p}(t, f) = \int_{-\infty}^{+\infty} x(\tau)K_p(\tau, f)h(\tau - t)d\tau \quad (1)$$

where x_p is the p th order FrFT of the signal $x(\tau)$, τ is the integral variable, t and f represent the time and frequency variables of the signal, respectively, $h(\tau - t)$ is a weighted window function, and $K_p(\tau, f)$ represents the kernel function of FrFT, replacing the kernel $\exp(j\omega\tau)$ of the Gabor transform. Equation (1) also can be regarded as the clockwise rotation angle α of the time-frequency plane:

$$GT_{x_p}(t, f) = GT_x(u \cos \alpha - v \sin \alpha, u \sin \alpha + v \cos \alpha) = R_\alpha\{GT_x(t, f)\} \quad (2)$$

where R_α represents the angle α rotation operator; u and v are the new coordinate axes obtained by representing the clockwise rotation angle $\alpha = p\pi/2$ of the time-frequency plane.

The two-dimensional FrGT transform is considered as the extension of one-dimensional FrGT, containing four variables (x, y, u, v), where x and y are spatial coordinates, and the time-frequency spectrum becomes four-dimensional. The expression of the two-dimensional FrGT transform is computed as

$$\begin{aligned} GT_{p_1, p_2}(x, y, u, v) &= \int_{-\infty}^{+\infty} \int_{-\infty}^{+\infty} f(\tau, \eta)K_{p_1, p_2}(\tau, \eta, u, v)h(\tau - x, \eta - y)d\tau d\eta \\ &= \int_{-\infty}^{+\infty} \int_{-\infty}^{+\infty} \frac{1}{2\pi}f(\tau, \eta)K_{p_1, p_2}(\tau, \eta, u, v)\exp\left(-\left[\frac{(\tau - x)^2}{2} + \frac{(\eta - y)^2}{2}\right]\right)d\tau d\eta \end{aligned} \quad (3)$$

where $f(\tau, \eta)$ represents the image, τ and η are the spatial domain variables, u and v are the frequency domain variables, $h(x, y)$ represents the Gaussian window function, and $K_{p_1, p_2}(\tau, \eta, u, v)$ is the kernel of two-dimensional FrFT and has the separability, defined as

$$\begin{aligned} K_{p_1, p_2}(\tau, \eta, u, v) &= \frac{\sqrt{1 - j\cot \alpha}\sqrt{1 - j\cot \beta}}{2\pi} \exp\left(\frac{j(\tau^2 + u^2)}{2\tan \alpha} - \frac{j\tau u}{\sin \alpha}\right) \exp\left(\frac{j(\eta^2 + v^2)}{2\tan \beta} - \frac{j\eta v}{2\sin \beta}\right) \\ &= K_{p_1}(\tau, u)K_{p_2}(\eta, v) \end{aligned} \quad (4)$$

where $\alpha = p_1\pi/2$ and $\beta = p_2\pi/2$ represent the two-dimensional rotation angles. The Gabor transform is a special case of the short-time Fourier transform, when the window is a Gaussian function. The Gaussian function is also separable. Based on this particularity, the two-dimensional Gabor transform can be expressed as a cascade of two one-dimensional representations by transforming (3) and changing

the order of integration, shown as

$$\begin{aligned} \text{GT}_{p_1,p_2}(x, y, u, v) &= \int_{-\infty}^{+\infty} \int_{-\infty}^{+\infty} \frac{1}{2\pi} f(\tau, \eta) K_{p_1}(\tau, u) K_{p_2}(\eta, v) \exp\left(-\frac{(\tau-x)^2}{2}\right) \exp\left(-\frac{(\eta-y)^2}{2}\right) d\tau d\eta \\ &= \int_{-\infty}^{+\infty} \left[\int_{-\infty}^{+\infty} \frac{1}{\sqrt{2\pi}} f(\tau, \eta) K_{p_2}(\eta, v) \exp\left(-\frac{(\eta-y)^2}{2}\right) d\eta \right] \frac{1}{\sqrt{2\pi}} K_{p_1}(\tau, u) \exp\left(-\frac{(\tau-x)^2}{2}\right) d\tau. \end{aligned} \tag{5}$$

It can be seen from (5) that FrGT of the image can be carried out along one direction first, and then along another direction. Finally, the discrete form of two-dimensional FrGT can be expressed as

$$\begin{aligned} \text{GT}_{p_1,p_2}\left(m, n, \frac{k}{KT_x}, \frac{q}{QT_y}\right) &= \\ \sum_{\tau=0}^{M-1} \sum_{k=0}^{K-1} \left[\sum_{\eta=0}^{N-1} \sum_{q=0}^{Q-1} f(\tau, \eta) K_{p_2}\left(\eta, \frac{q}{QT_y}\right) \frac{1}{\sqrt{2\pi}} \exp\left(-\frac{(\eta-n)^2}{2}\right) \right] & K_{p_1}\left(\tau, \frac{k}{KT_x}\right) \frac{1}{\sqrt{2\pi}} \exp\left(-\frac{(\tau-m)^2}{2}\right) \end{aligned} \tag{6}$$

where K and Q are the sampling numbers in the fractional domain; M and N are the sizes of the image; T_x and T_y represent the sampling intervals in the spatial domain; m and n are the discrete sampling sequence numbers corresponding to M and N , respectively; k and q are the discrete sampling sequence numbers corresponding to K and Q , respectively.

2.2. Optimal window function design

The Gabor transform is a special case when the window function is Gaussian in the short-time Fourier transform. In order to avoid clutter and distortion, the design of the window function is of great significance. The time-frequency bandwidth product (TBP) is an important measure of time-frequency aggregation [18]. Due to the influence of the uncertainty principle, for example, there is a mutual constraint relationship between the minimum value of TBP and the time-frequency resolution, it is necessary to design an optimal window function to solve the problem.

As shown in (2), TBP of x_p will change in different orders. The generalized time-bandwidth product (GTBP) [19,20] is defined as

$$\text{GTBP}\{x(t)\} = \min_{0 \leq p < 4} \text{TBP}\{x_p(t)\}. \tag{7}$$

According to (7), the optimal order can be obtained from GTBP, when the fractional signals have minimum TBP. The definition of the optimal order is shown as

$$p_{\text{opt}} = \underset{p}{\text{argmin}} \text{TBP}\{x_p(t)\}. \tag{8}$$

The rotation angle corresponding to the optimal order is $\alpha = p_{\text{opt}}\pi/2$. The time bandwidth and frequency bandwidth of the fractional signal $x_p(t)$ are calculated as

$$T_{x_p} = \frac{[\int (u - \eta_u)^2 |x_p(t)|^2 du]^{1/2}}{\|x_p\|^2} \tag{9a}$$

$$B_{x_p} = \frac{[\int (v - \eta_v)^2 |x_p(f)|^2 dv]^{1/2}}{\|x_p\|^2} \tag{9b}$$

where η_u and η_v are the average values of fractional time and frequency domain, respectively.

The optimal window function at the p th order can be obtained by

$$h_{\text{opt},p}(t) = \text{FrFT}(\exp(-\pi t^2 B_p / T_p)) \tag{10}$$

$$T_p = \sqrt{T_{x_p}^2 + T_h^2} \tag{11}$$

$$B_p = \sqrt{B_{x_p}^2 + B_h^2} \tag{12}$$

where T_h is the time bandwidth, and B_h is the frequency bandwidth of $h(t)$.

2.3. Optimal order determination

The fractional time-frequency analysis is a kind of generalized time-frequency transforms. It can show the changing characteristics of the signal from the time domain to the frequency domain step by step. It can provide more choices for the time-frequency analysis of the signal to improve the performance of the analysis. Its advantages are that it can improve the time-frequency distribution, which is more sensitive to weak mutations, and can depict the target features more precisely. To achieve this effect, one of the key problems to be solved is how to determine the optimal transform order of FrGT.

According to (7) and (8), we confirm that GTBP can effectively improve time-frequency focusing and suppress clutter. In this paper, we propose to determine the optimal order by searching for the peak energy of the target area. Before counting the energy of the target area, the isolated clutter points are filtered first, and then the energy of the target area of the optimal window FrGT spectrum at each order is counted. Finally, the corresponding order of the maximum energy is found, that is, the optimal order. The search method can be expressed as

$$P = \operatorname{argmax}_p \{ \operatorname{sum}_{\text{ROI}} (\operatorname{Energy}(x_p)) \} \tag{13}$$

where $\operatorname{Energy}(x_p)$ represents the energy of FrGT with different orders, and the subscript ROI stands for the target area.

2.4. EAG feature

The optimal window function is designed to obtain the best time-frequency aggregation. The optimal transform order is selected to compensate for the phase information and fine detect the weak edge information. The extraction and analysis of the optimal time-frequency spectrum features are the key to completing the accurate detection of ground targets. The optimal time-frequency spectrum is obtained by designing the optimal window function, searching for the optimal order, and finally performing the optimal FrGT transform.

In this paper, the local energy focusing analysis is used to extract the EAG feature from the optimal time-frequency spectrum. The detection performance of weak targets with this feature is better. The flow chart of this method in SAR image detection is shown in Fig. 1, and is described in detail below:

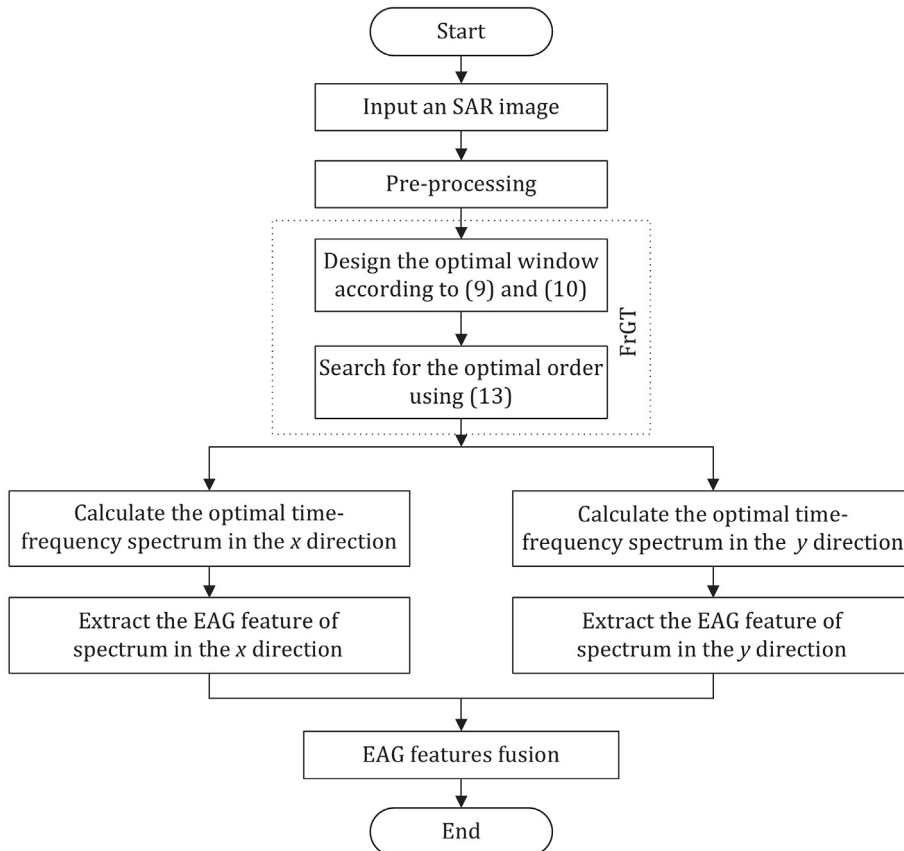


Fig. 1. Flowchart of the proposed algorithm for detecting targets in SAR images.

- 1) Input an SAR image of $m \times n$ and de-noise with the Lee filter.
- 2) Design the optimal window function according to (10), search for the optimal order according to (13), and take the optimal FrGT transform on the two-dimensional image to obtain the optimal time-frequency spectrum.
- 3) Extract the optimal time-frequency spectrum in the column direction, and process the neighborhood frequency distribution corresponding to each location. There are n -channel signals in common, so the spatial local energy focusing characteristics are analyzed in detail.
- 4) The frequency f_{\max} corresponding to the maximum peak value, Max, of each channel signal is extracted, and then the frequency f_{\min} corresponding to 0.1Max is found. The energy value corresponding to the attenuation sample points between f_{\min} and f_{\max} is fitted by the least square principle to obtain EAG features. At the beginning of the fitting process, in order to prevent from falling into the local minimum, the derivative of the frequency distribution corresponding to each location is first calculated. The sample points with high-frequency partial derivatives greater than 0 are judged. The points with the growth trend are eliminated, and the attenuation sample points are retained. The sample points, as many as possible, are selected for fitting. The least square method of curve fitting ensures that the absolute value of each distance difference is very small by minimizing

$$\min \sum_i [p(f_i) - y_i]^2 \quad (14)$$

where f_i represents the frequency f corresponding to the time-frequency plane, and y_i represents the energy value corresponding to each frequency. For given data points $\{f_i, y_i\}, (i = 1, 2, \dots, n)$, in the geometric sense, it is to seek the minimum sum of squares of distances from the point sets in the curve $y = p(f_i)$.

- 5) Extract the optimal time-frequency spectrum of the SAR image in the row direction, repeat step 4), and get the EAG profile of the row direction.
- 6) Finally, the optimal EAG features profile is obtained by synthesizing the row direction feature profile, and the target detection is completed.

3. Algorithm testing and simulation

3.1. Optimal window function

As mentioned above, the Gabor transform is the windowed Fourier transform essentially. A reasonable design of the window function can reduce clutter and improve the time-frequency aggregation and detection performance. One of the key technologies of the proposed algorithm is to design the optimal window function by using GTBP. As shown in Fig. 2, the detection of the chirp signal is carried out by using the optimal window function designed by GTBP compared with the Gabor transform. The chirp signal is shown as

$$x = \cos(2\pi t) \exp(j\pi t^2). \quad (15)$$

Equation (15) is selected to test the algorithm.

Fig. 2 shows the time-frequency aggregation improvement of the Gabor transform using the optimal window function designed in the GTBP criterion. Fig. 2 (a) is the waveform of the chirp signal. The range of time is $[-8 \text{ s}, 8 \text{ s}]$, and the sampling frequency is 16 Hz. Fig. 2 (b) is the Gabor transform with the ordinary Gaussian window, which detects the instantaneous energy change of the chirp signal, but the time-frequency aggregation is poor, so it cannot meet the requirements of accurate detection. Fig. 2 (c) is the result of the Gabor transform using the optimal window function. The time-frequency aggregation has been significantly improved, the detection accuracy also has been improved, and the clutter has been reduced, which lays a good foundation for feature extraction.

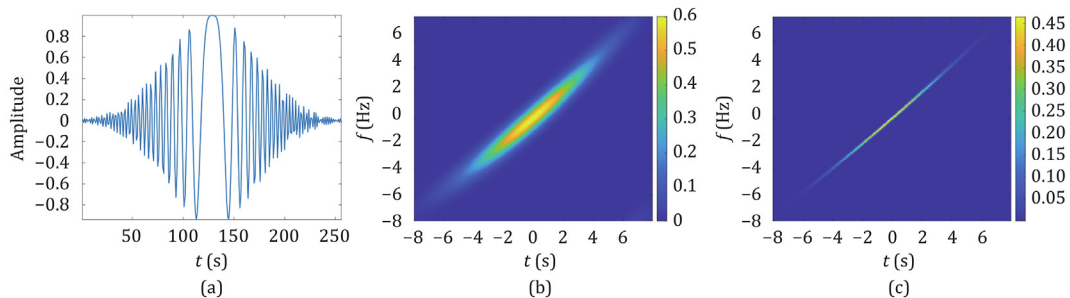


Fig. 2. Comparison of time-frequency aggregation between different transforms: (a) chirp signal, (b) Gabor transform, and (c) Gabor transform with the optimal window function.

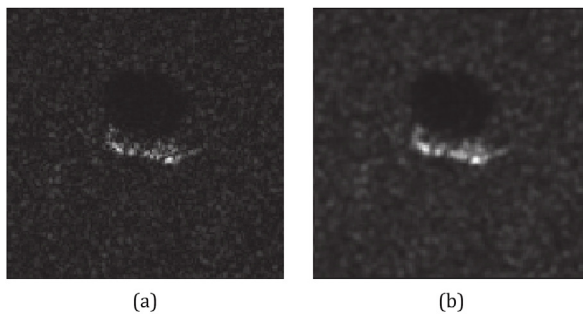


Fig. 3. SAR image and pre-processed image: (a) BTR image and (b) pre-processed image after filtering.

3.2. Optimal time-spectrum detection

In order to verify the advantage of optimal FrGT in SAR ground target detection, we use the image of the BTR_60 armored vehicle target in the Moving and Stationary Target Acquisition and Recognition (MSTAR) image database as the test image. Fig. 3 (a) is the BTR target image and Fig. 3 (b) is a pre-processed image. The original SAR image is filtered by using the Lee filter to reduce the influence of noise. However, filtering also weakens the target area, so some details become weak and are difficult to detect.

Fig. 4 compares the FrGT results of different windows and fractional orders for the targets shown in Fig. 3. Fig. 4 (a) shows the detection result of the Gabor transform extracting the EAG feature with the ordinary Gaussian window. It can be seen that there is much clutter in the target area and the time-frequency aggregation is poor. Fig. 4 (b) is the detection result of extracting spectrum features by using the Gabor transform with GTBP to design the optimal window function. The time-frequency aggregation is greatly improved and the clutter is reduced, but the weak edge feature is not detected. Fig. 4 (c) shows the detection result with the 1.5-order optimal window fractional spectral features, which does not detect the weak edge features of the target. And there is distortion. Fig. 4 (d) is the detection result using FrGT spectral characteristics with the optimal order window. Compared with the detection results of Figs. 4 (a)–(c), in Fig. 4 (d), the target area is more accurate in describing the shape of the target. Many weak edge features are also detected, and there is almost

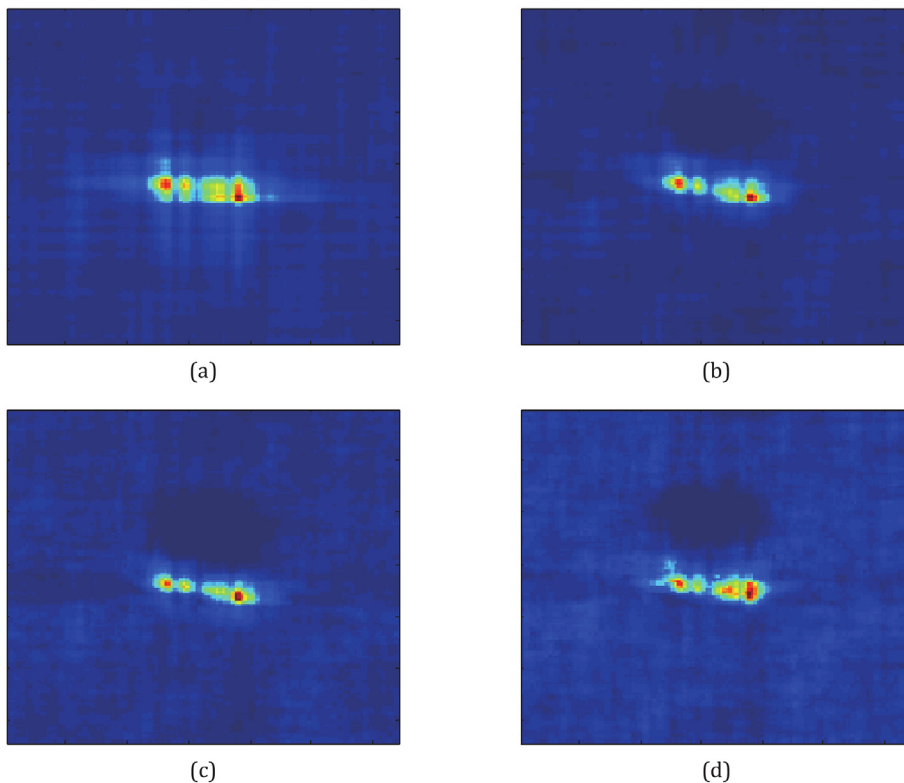


Fig. 4. Comparison of FrGT spectrum feature with different parameters: (a) Gabor, (b) Gabor with optimal window, (c) FrGT with 1.5 order, and (d) FrGT with optimal order.

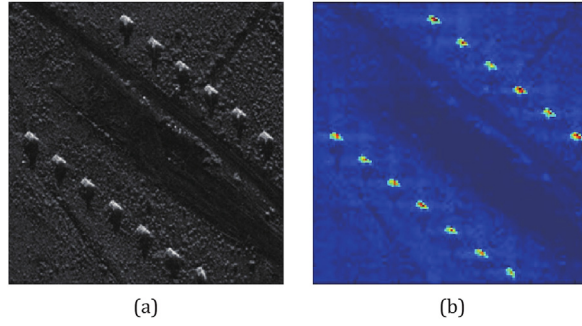


Fig. 5. Detection on small SAR ground targets: (a) test image and (b) result.

Table 1
Evaluation of detection performance.

Dataset	Average detection rate (%)	Average false alarm rate (%)
BTR_60	95.7	2.1
T72	92.1	1.1
BMP	95.3	1.6

no clutter. The weak edge information obliterated by noise is accurately detected, and the contrast between the background, shadow, and target area is increased, which is convenient to segment the shadow and target region, providing more feature selection for target recognition.

3.3. Application and results analysis

Fig. 5 shows the detection results for small SAR ground targets. There are 13 ground military targets in Fig. 5 (a). Fig. 5 (b) is a feature profile obtained by extracting the EAG feature of the optimal time-frequency spectrum. It can be seen that all the targets are detected, and the shapes of the targets are delicately depicted.

In order to quantitatively analyze the detection performance of this method, a total of 210 SAR images in seven types of BTR_60, T72, and BMP in the MSTAR image database are tested, and the detection rate and false alarm rate of each image are calculated according to (16) and (17). Finally, the average detection rate and false alarm rate of all sample image detection results are given in Table 1, measuring the algorithmic performance at the pixel level.

The target detection rate (R_d) is defined as

$$R_d = \frac{N_{dt}}{N_{tg}} \quad (16)$$

where N_{dt} is the number of target feature points by comparing the pixel position of the target area with the position of the feature points detected, and N_{tg} is the total number of pixels in the target area.

The false alarm rate (R_a) is defined as

$$R_a = \frac{N_{al}}{N_{clutter}} \quad (17)$$

where $N_{clutter}$ is the total number of pixels in the image clutter background, and N_{al} is the number of pixels in the detected non-target area.

As listed in Table 1, the proposed algorithm detects different kinds of targets with different resolution values, perspectives, and types in the MSTAR database. The average detection rate is larger than 92%, and the average false alarm rate is also kept at a low level. It proves that this method can detect the weak edge features of SAR targets accurately and analyze their characteristics carefully.

4. Conclusions

In order to improve the time-frequency resolution, the fractional time-frequency analysis of the one-dimensional signal is extended to the two-dimensional image signal by using the rotational characteristics of FrFT on the time-frequency plane. By designing the optimal window function of the Gabor transform, the detection performance of the time-frequency analysis method is improved. By searching for the optimal order, this method not only has the characteristics of the general time-frequency analysis method, but also improves the time-frequency distribution of the image. The EAG feature of the time-frequency spectrum is sensitive to weak mutations

and is suitable for target detection in SAR images with a low signal-to-noise ratio. The simulation results of a large number of SAR images show that the proposed method can provide the accurate analysis for SAR images and get better detection results.

Funding

This work was supported by the Natural Science Foundation of Sichuan Province of China under Grant No. 2022NSFSC40574, and partially supported by the National Natural Science Foundation of China under Grants No. 61571096 and No. 61775030.

Declaration of competing interest

The authors declare no conflicts of interest.

References

- [1] Z.-Z. Li, L. Tian, W. Zhang, Y.-H. Zhang, G. Jin, Dim moving target detection method based on time-frequency analysis, *High Power Laser and Particle Beams* 23 (9) (Sept. 2011) 2292–2296.
- [2] V. Namias, The fractional order Fourier transform and its application to quantum mechanics, *IMA J. Appl. Math.* 25 (3) (Mar. 1980) 241–265.
- [3] H.M. Ozaktas, O. Arikan, M.A. Kutay, G. Bozdagit, Digital computation of the fractional Fourier transform, *IEEE T. Signal Proces.* 44 (9) (Sept. 1996) 2141–2150.
- [4] H. Chen, Z.-M. Peng, J. Wang, Y.-G. Hong, W. Zou, Spectral decomposition of seismic signal based on fractional Gabor transform and its application, *Chinese J. Geophys.-CH* 54 (3) (Mar. 2011) 867–873.
- [5] S. Sinha, P.S. Routh, P.D. Anno, J.P. Castagna, Spectral decomposition of seismic data with continuous-wavelet transform, *Geophysics* 70 (6) (Nov. 2005) 19–25.
- [6] Z.-M. Peng, J. Zhang, F.-M. Meng, J. Dai, Time-frequency analysis of SAR image based on generalized S-transform, in: *Proc. of Intl. Conf. on Measuring Technology and Mechatronics Automation, Zhangjiajie, 2009*, pp. 556–559.
- [7] S.-C. Pei, J.-J. Ding, The generalized radial Hilbert transform and its applications to 2D edge detection (any direction or specified directions), in: *Proc. of IEEE Intl. Conf. on Acoustics, Speech, and Signal Processing, Hong Kong, 2003*, pp. 357–360.
- [8] E. Sejdić, I. Djurović, L. Stanković, Fractional Fourier transform as a signal processing tool: An overview of recent developments, *Signal Process.* 91 (6) (Jun. 2011) 1351–1369.
- [9] S.-S. He, Y.-Y. Jiang, J.-Y. Zheng, A novel image denoising method in 2D fractional time-frequency domain, *Applied Mechanics and Materials* 734 (Feb. 2015) 586–589.
- [10] J.-B. Long, H.-B. Wang, P. Li, H.-S. Fan, Applications of fractional lower order time-frequency representation to machine bearing fault diagnosis, *IEEE-CAA J. Automatic.* 4 (4) (Oct. 2017) 734–750.
- [11] X.-L. Chen, X.-H. Yu, J. Guan, J. Zhang, Detection and extraction of marine target with micromotion via short-time fractional Fourier transform in sparse domain, in: *Proc. of IEEE Intl. Conf. on Signal Processing, Communications and Computing, Hong Kong, 2016*, pp. 1–5.
- [12] W. Qian, Y. Fei, Z. Yi, C. En, Gabor Wigner transform based on fractional Fourier transform for low signal to noise ratio signal detection, in: *Proc. of OCEANS, Shanghai, 2016*, pp. 1–4.
- [13] Y.-Q. Wang, Z.-M. Peng, X.-Y. Wang, Y.-M. He, Matching pursuit-based sliced Wigner higher order spectral analysis for seismic signals, *IEEE J.-STARS* 10 (8) (Aug. 2017) 3821–3828.
- [14] J.-B. Long, H.-B. Wang, D.-F. Zha, P. Li, H.-C. Xie, L.-L. Mao, Applications of fractional lower order S transform time frequency filtering algorithm to machine fault diagnosis, *PLoS One* 12 (4) (Apr. 2017) e0175202:1–24.
- [15] L. Tian, Z.-M. Peng, Determining the optimal order of fractional Gabor transform based on kurtosis maximization and its application, *J. Appl. Geophys.* 108 (Sept. 2014) 152–158.
- [16] A. Akan, E. Önen, A discrete fractional Gabor expansion for multi-component signals, *AEU-Int. J. Electron. C.* 61 (5) (May 2007) 279–285.
- [17] C. Candan, M.A. Kutay, H.M. Ozaktas, The discrete fractional Fourier transform, *IEEE T. Signal Proces.* 48 (5) (May 2000) 1329–1337.
- [18] L. Durak, O. Arikan, Short-time Fourier transform: Two fundamental properties and an optimal implementation, *IEEE T. Signal Proces.* 51 (5) (May 2003) 1231–1242.
- [19] Y.-P. Chen, Z.-M. Peng, A novel optimal STFrFT and its application in seismic signal processing, in: *Proc. of Intl. Conf. on Computational Problem-Solving, Leshan, 2012*, pp. 328–331.
- [20] J.-T. Yang, Z.-M. Peng, SAR target recognition based on spectrum feature of optimal Gabor transform, in: *Proc. of Intl. Conf. on Communications, Circuits and Systems, Chengdu, 2013*, pp. 230–234.



Ling-Bing Peng received the B.S. degree in communications engineering from University of Electronic Science and Technology of China (UESTC), Chengdu, China in 2012, and the Ph.D. degree in communications and information systems from UESTC in 2020. She is currently a postdoctoral researcher with the Institute of Optics and Electronics, Chinese Academy of Sciences, Chengdu, China. Her research interests include signal processing, image processing, and target recognition and tracking.



Yu-Qing Wang received the Ph.D. degree from UESTC in 2018. She is currently working as a research assistant with the Changchun Institute of Optics, Fine Mechanics and Physics, Chinese Academy of Sciences, Changchun, China. Her research interests include signal processing, time-frequency analysis, seismic attribute analysis, and fluid identification.



Ying-Pin Chen received his B.S. degree in electronic science and technology from Fuzhou University, Fuzhou, China in 2009. He received his M.S. and Ph.D. degrees in signal and information processing from UESTC in 2013 and 2019, respectively. He is now an associate professor with the School of Physics and Information Engineering, Minnan Normal University, Zhangzhou, China, and a postdoctoral researcher with UESTC. His research interests include time-frequency analysis, compressed sensing, and convex optimization.



Zhen-Ming Peng received the Ph.D. degree in geo-detection and information technology from Chengdu University of Technology, Chengdu, China in 2001. From 2001 to 2003, he was a postdoctoral researcher with the Institute of Optics and Electronics, Chinese Academy of Sciences. Currently, he is a professor with UESTC and is the Head of the Laboratory of Imaging Detection and Intelligent Perception, UESTC. His research interests include image processing, radar signal processing, and target recognition and tracking.